Received: 28 July 2021 | Revised: 3 January 2022 | Accepted: 4 January 2022

DOI: 10.1002/ptr.7396

RESEARCH ARTICLE

WILEY

Kaempferol exerts a neuroprotective effect to reduce neuropathic pain through TLR4/NF-κB signaling pathway

Shiquan Chang[1] | Xin Li[1] | Yachun Zheng[1] | Huimei Shi[1] | Di Zhang[1] | Bei Jing[1] | Zhenni Chen[1] | Guoqiang Qian[2] | Guoping Zhao[1]

[1]College of Traditional Chinese Medicine, Jinan University, Guangzhou, China

[2]College of Traditional Chinese Medicine, Guangdong Pharmaceutical University, Guangzhou, China

Correspondence
Guoping Zhao, College of Traditional Chinese Medicine, Jinan University, Guangzhou 510630, China.
Email: tguo428@jnu.edu.cn

Guoqiang Qian, College of Traditional Chinese Medicine, Guangdong Pharmaceutical University, Guangzhou, China.
Email: gqqian1@163.com

Funding information
National Natural Science Foundation of China, Grant/Award Number: 81874404

Abstract

Switching microglial polarization from the M1 to M2 phenotype is a promising therapeutic strategy for neuropathic pain (NP). Toll-like receptor 4 (TLR4) is activated by lipopolysaccharide (LPS). Uncontrolled activation of TLR4 has been proven to trigger chronic inflammation. Kaempferol, a dietary flavonoid, is known to have anti-inflammatory properties. This study is aimed to investigate the analgesic and anti-inflammatory effects and the underlying mechanisms of kaempferol, which were explored with an NP model in vivo and LPS-induced injury in microglial BV2 cells in vitro. The levels of proinflammatory cytokines were evaluated. H&E staining and immunohistochemistry were used to assess the sciatic nerve condition after chronic constriction injury surgery. Western blotting and immunofluorescence were used to determine whether TLR4/NF-κB signaling pathway plays a major role in kaempferol-mediated alleviation of neuroinflammation. Quantitative real-time polymerase chain reaction and flow cytometry were used to examine the modulator effect of kaempferol on microglial M1/M2 polarization. We found that kaempferol treatment can significantly reduce NP and proinflammatory cytokine production. Kaempferol attenuated the activation of TLR4/NF-κB pathways in LPS-activated BV2 cells. The analgesic effects of kaempferol on NP may be due to inhibition of microglia activation and switching the M1 to M2 phenotype.

KEYWORDS
kaempferol, microglial, neuroinflammation, NF-κB, TLR4

1 | INTRODUCTION

The classification of chronic pain falls into three broad categories: pain owing to tissue disease or damage (nociceptive pain, such as osteoarthritis), pain caused by somatosensory system disease or damage (neuropathic pain [NP]), and coexistence of nociceptive and NP (mixed

Abbreviations: CCI, chronic constriction injury; ELISA, enzyme-linked immunosorbent assay; ERK, extracellular signal-regulated kinase; iNOS, inducible nitric oxide synthase; JNK, c-Jun N-terminal kinases; LPS, lipopolysaccharide; MAPK, mitogen-activated protein kinases; NF-κB, nuclear factor-kappa B; NP, neuropathic pain; PGE2, prostaglandin E2; PMWT, paw mechanical withdrawal threshold; PTWL, paw thermal withdrawal latency; TLR4, Toll-like receptor 4; TNF-α, tumor necrosis factor-α.

pain) (Baron, 2006). NP develops due to lesions or disease affecting the somatosensory nervous system either in the periphery or centrally, yet the clinical manifestation of the pain is similar across the different neuropathic syndromes and causes (Baron, Binder, & Wasner, 2010; Colloca et al., 2017). NP greatly reduces the quality of life of the patients. Currently available treatments exhibit only moderate efficacy and have troubling side effects. Numerous studies have reported the effectiveness of tricyclic antidepressants, gabapentin, lamotrigine, phenytoin, pregabalin, opioids, and tramadol for treating painful sensory neuropathy (Attal, 2001; Harden, 1999). These therapies reduce pain by 30–50% but are accompanied by side effects, such as sedation.

Substantial evidence suggests that neuroinflammation plays an important role in the development of NP (Lurie, 2018). Microglial, resident macrophage-like immune cells in the central nervous system, have been regarded as primary mediators of neuroinflammation (Suzumura, 2013). In vivo studies have demonstrated that inhibition of overactivated microglial can attenuate NP, suggesting that microglial may represent a potential therapeutic target to combat NP (Dai et al., 2020; Inoue & Tsuda, 2018). Microglial can be activated in a polarizing manner into a classical phenotype (pro-inflammatory, M1) or an alternative phenotype (anti-inflammatory, M2). The M1 phenotype exacerbates neurotoxicity, whereas the M2 phenotype exerts neuroprotection (Xu et al., 2017). Therefore, shifting the polarization of microglial from the M1 phenotype toward the M2 phenotype may be a promising strategy for the treatment of neuroinflammatory disorders.

Several signaling molecules, including Toll-like receptor 4 (TLR4)/nuclear factor-kappa B (NF-κB) and TREM2, are critical to the modulation of microglial activation and neuroinflammation (J. Zhang et al., 2019). TLR4 is an important pattern recognition receptor that activates both innate and adaptive immune cells. TLR4 activation by lipopolysaccharide (LPS) or damage-associated molecular patterns leads to the production of pro-inflammatory cytokines. TLR4 is predominantly expressed in the microglial of the brain and is stimulated by appropriate ligands, including LPS. TLR4 ultimately activates various downstream signal transduction pathways, including the NF-κB signaling pathway, thus leading to transcription of a series of pro-inflammatory genes that induce neuroinflammation and neurodegeneration (Lee et al., 2017). Notably, LPS-activated microglial cells have been suggested to be a good cellular model to test the efficacy of therapeutic compounds for neuroinflammatory disorders (Le et al., 2001).

Considerable attention has focused on identifying naturally occurring neuroprotective substances that may be promising therapeutics for NP. Flavonoids are involved in the inhibition of various enzymes which provoke the inflammation process. Kaempferol (3, 4′, 5, 7,tetrahydroxyflavone), a well-characterized natural polyphenol and one of the most common dietary flavonoids, is commonly found in tea, broccoli, grapefruit, and other various plant sources. It is known to have antioxidative and anti-inflammatory properties.

Therefore, this study was designed to investigate whether kaempferol exerts neuroprotection via inhibition of microglial activation and the subsequent neuroinflammation.

2 | MATERIALS AND METHODS

2.1 | Reagents

Kaempferol (K107144, HPLC ≥98%) was purchased from Shanghai Aladdin Biochemical Technology Co., Ltd. Pregabalin (Pfizer, Imported drug number H20150620) for in vivo experiments was obtained from Guangzhou Overseas Hospital, First Affiliated Hospital of Jinan University. Lipopolysaccharide 055:B5, TAK-242, JSH-23 (L2880, S80562, and M134534, respectively) and cell counting kit-8 (96992) were purchased from Guangzhou Yiyou Biotechnology Biological Co., Ltd. PageRμLer Prestained Protein Ladder and Marker (P12083) was obtained from Shanghai Bioscience Technology Co., Ltd (China). The polyvinylidene fluoride (PVDF) membrane was captured from Millipore (Billerica, USA). Radioimmunoprecipitation assay (RIPA) was purchased in Guangzhou Dingguo Biological Co., Ltd. (China). SYBR Green Premix qPCR kit, Evo M-MLV RT Mix Kit, and RNase-free water (AG11701, AG11728, and AG11012, respectively) were obtained from Accurate Biotechnology Co., Ltd. ELISA kits of IL1β (MM-0047R1), IL6 (MM-0190R1), IL10 (MM-0195R11), LPS (MM-0647R1), PGE2 (MM-0068R1), and TNF-α (MM-0180R1) were purchased from MEIMIAN Industrial Co., Ltd. (CHINA). The antibodies used were as following: anti-TLR4 (505258, ZEN BIO), anti-β-actin (380624, ZEN BIO), anti-NF-κB p65(A5075, BIMAKE), anti-JNK (A5005, BIMAKE), anti-ERK (A5029, BIMAKE), anti-phospho-ERK (A5036, BIMAKE), anti-Iba1 rabbit recombinant mAb (A5595, BIMAKE), anti-p38 MAPK (8690S, CST), anti-phospho-p38MAPK (4511S, CST), anti-phospho-SARK/JNK (T183/Y185) (4668, CST), anti-S100b (GB11359, Servicebio), anti-Histone3 (GB11026, Servicebio), secondary antibody (E030120-02, EARTH), APC anti-mouse CD206 (MMR) (141708, Biolegend), PE anti-mouse CD32(Fcgr2) (156404, Biolegend). Phosphatase inhibitor cocktail 1 was purchased from Wuhan Servicebio Biological Technology. Primary antibody diluent, secondary antibody dilution, WB transfer solution, WB electrophoresis solution, and immunol fluorescence staining kit were purchased from Beyotime Biotechnology (Shanghai, China). Fixation buffer (420801) and intracellular staining perm wash buffer (421002) were purchased from Dakewe Biotech Co., Ltd. (Shenzhen, China).

2.2 | NP model

A rat model of NP was induced by chronic constriction injury (CCI) as described in our previous study (D. Zhang, Sun, et al., 2020). First, we injected pentobarbital sodium (2%, 50 mg/kg) into the rats. Then, the rat limbs were fixed, and we exposed the right sciatic nerve. The right sciatic nerve was ligated with 4.0 sutures at 4 sites approximately 1 mm apart under a microscope. During this time, we observed a small twitch in the operated hind limb. Then, gentamicin (10 mg/ml, i.m.) was injected into the right biceps femoris. Increased sensitivity of the injured hind paw to pain after surgery indicated successful modeling of chronic neuralgia. The rats in the sham group underwent cutting and suturing of the skin and muscles without nerve ligation.

2.3 | In vivo drug treatment

A total of 32 8-week-old adult male Sprague–Dawley rats (220–280 g) acquired from the experimental center of Beijing Huafukang Co. Ltd. were used in this study. All rats were acclimated for 10 days before any experimental procedure. All animal experiments were approved (approval number IACUC-20201223-07) by the Committee on the Ethics of Animal Experiments and followed the guidelines of the Institute of Laboratory Animal Science, Jinan University. Rats were housed in a temperature-controlled environment and maintained on a 12-hr light/dark cycle with food available ad libitum. The rats were randomly divided into 4 groups: (a) sham operation group (Sham)—the sciatic nerve of the right hind limb of the rats was exposed, without ligation, the incisions were sutured layer by layer, and an intragastrical (i.g.) injection of normal saline was administered daily; (b) CCI model group (CCI)—the CCI model was established, and then the rats were intragastrically administered with normal saline daily; (c) pregabalin treatment group—the CCI model was established, and then the rats were intragastrically administered with 10 mg/kg of pregabalin every day; (d) kaempferol treatment group (Kae)—the CCI model was established, and then the rats were intragastrically administered with 60 mg/kg of kaempferol every day (Li et al., 2019). The injection was performed manually over a 30 s period in a single injection volume of 5 ml/kg. Each group was orally administered respective treatments once per day for 21 days. At the end of the 21-day period, the rats were fasted for 12 hr and then given euthanization for blood, right sciatic nerve, spinal dorsal horn, liver, and kidney.

2.4 | Behavior assessments

The values of paw mechanical withdrawal threshold (PMWT) and paw thermal withdrawal latency (PTWL) were measured 1 day before surgery as preoperative values (namely, Day 0). The two indicators were tested again on Days 1, 4, 7, 14, and 21 after surgery. Briefly, the rats were individually placed in a plastic chamber ($7 \times 9 \times 11$ cm^3) with a smooth glass surface, 1 mm in thickness, on the bottom for PTWL measurement. The heat source was located below the glass surface. The rats underwent a familiarization period of 30 min before the behavior tests. The heat was directed toward the ipsilateral paws of the rats. To avoid tissue damage, an automatic 20s cut-off was set. The procedure was repeated three times on each ipsilateral paw, with a 5 min interval between each heat treatment (Hargreaves, Dubner, Brown, Flores, & Joris, 1988). For the PMWT measurement, the rat was placed in a transparent Plexiglass cube, 30 cm on each side, on a shelf made of wire mesh with small holes. The rat's rapid foot-lifting response during the stimulation time or when the Von-Frey is recorded as a positive reaction. The average value of the pressure value corresponding to Von-Frey is used as the foot lift threshold. We used 26 g Von-Frey as the maximum folding force. When the measured value was greater than 26 g, we record 26 g (Mitrirattanakul et al., 2006). All behavioral assessments were scored by individuals who were blinded to experimental treatments.

2.5 | Hematoxylin–eosin staining

We incubated the ligated sciatic nerve tissues in 4% paraformaldehyde for 1 day, embedded them in paraffin, and sectioned them at a thickness of 3 μm. The sections were deparaffinized in xylene and rehydrated through 100, 90, 80, and 70% ethanol. Then, we rinsed the sections in PBS for 5 min. After staining, two pathologists who were blinded to the experimental design observed staining images and assessed tissue damage.

2.6 | ELISA for the determination of cytokine levels

An abdominal aorta blood sample was centrifuged at 3000 rpm for 15 min at 4°C. We obtained 800 μl of the supernatant, which was immediately transferred to a clean sample tube and stored at −20°C until ELISA measurement. The levels of various cytokines include tumor necrosis factor (TNF)-α, interleukin (IL)-1β, IL-6, IL-10, LPS, and prostaglandin E2 (PGE2) were measured by ELISA according to the manufacturer's instructions. We used a microplate reader (BioTek Corporation, USA) to measure the optical density (OD).

2.7 | Immunohistochemical determination of the expression of IBA-1, S100b, and TLR4 in the sciatic nerve

Right sciatic nerves (from 3 rats) were fixed in 4% paraformaldehyde for 24 hr. After being washed with PBS twice and dehydrated, they were embedded in paraffin, then sliced into 3 μm-thick sections. Sections from the individual animals were incubated in sodium citrate antigen repair solution (1:1000 dilution, pH = 6) and blocked in a 3% bovine serum albumin solution for 30 min. The sections were incubated with primary anti-Iba1, anti-S100b, and anti-TLR4 antibodies overnight at 4°Cand then with the corresponding secondary antibody. The sections were rinsed with 0.1 M PB and followed by DAB. Finally, the slides were washed in distilled water, dehydrated, made transparent, and sealed with xylene. Images were captured under a bright-field microscope (Olympus) and observed at ×400 magnification. The positive cells were stained yellow-brown. Mean optical density was analyzed using Image-Pro Plus 6.0 (Media Cybernetics, Inc., Rockville, MD, USA). At least three random sections from each group were analyzed.

2.8 | In vitro cell culture and drug treatments

BV2 microglial cells were kindly provided by the Formula-pattern research center of the school of traditional Chinese medicine at Jinan University. The cell line used in the experiments was between passages 4 and 10. The cells were cultured in high glucose Dulbecco's modified Eagle's medium (Gibco, Grand Island, NY) containing 10% fetal bovine serum with antibiotics (penicillin and streptomycin) (1%) at 37°C in a 5%

CO_2 humidified atmosphere. After reaching 70% confluency, the cells were treated with LPS (1 μg/ml), kaempferol (10 μM, the dose of kaempferol that significantly attenuated cell toxicity was selected on the basis of CCK8 assay), and TAK-242 (10 μM) or JSH-23 (10 μM) for specific inhibition of the TLR4 and NF-κB, respectively. Kaempferol was dissolved in dimethyl sulfoxide (DMSO) and added to the cell culture medium to a final concentration of 0.01% DMSO. All the chemicals/drugs were incubated with the cells for 24 hr at 5% CO_2 and 37°C.

2.9 | Cell viability assay

A CCK-8 assay was performed to evaluate the cell viability after kaempferol treatment. BV2 cells were incubated for 24 hr after plating in 96-well plates, and then treated with kaempferol of different concentrations of 5, 10, 50, 100, 200, 250, 300, 350 μM for 24 hr, then the culture medium was removed and replaced. After incubation for another 24 hr, CCK-8 solution (10 μl) was added to each well and further incubated for 1 hr. The absorbance of each well was measured at a wavelength of 450 nm on a microplate reader.

2.10 | Western blotting

The right spinal dorsal horn from rats was homogenized in RIPA buffer containing 1 mM phenylmethylsulfonyl fluoride (PMSF) and centrifuged at 14,000*g* for 20 min. Total protein from the BV2 cells was extracted in RIPA lysis buffer containing 1 mM PMSF and centrifuged at 13,000*g* for 20 min. The cell nuclear protein was obtained according to the nuclear protein extraction kit (Solarbio Science & Technology Co., Ltd, China). The supernatants were collected and subjected to the BCA assay (Solarbio, China) to determine their protein concentration and then separated them by SDS-PAGE followed by transferring the proteins from the gels to PVDF membrane and blocking the membranes with 5% skim milk. The membranes were incubated with the primary antibodies overnight at 4°C, washed with 1× TBST, and reacted with secondary antibodies for 1 hr. Luminescence was observed by spraying the membranes with a fluorescent solution, and the images were obtained using ChemiDoc MP Imaging System (BIO-RAD). Western blotting was performed with anti-TLR4 (1:1000), anti-p38 MAPK (1:1000), anti-p-p38 MAPK (1:1000), anti-JNK (1:1000), anti-p-JNK(1:1000), anti-ERK1/2 (1:1000), anti-p-ERK1/2 (1:1000), anti-Iba-1 (1:1000), or anti-β-actin (1:1000), anti-H3 (1:1000) followed by horseradish peroxidase-conjugated goat anti-rabbit secondary antibodies (1:10000). The densities of the bands were quantified using ImageJ, while graphs were generated by GraphPad Prism 8 software.

2.11 | Quantitative PCR (qPCR) assay

Total RNA was extracted from cells using TRIzol reagent (Invitrogen) and then used for reverse transcription using a cDNA Reverse Transcription Kit (Accurate Biotechnology, China). qRT-PCR was performed using a SYBR Green PCR Mix kit (Accurate Biotechnology) with specific primers synthesized by Tsingke Biotechnology Co., Ltd. (Beijing, China) on the BIO-RAD CFX96 Real-Time PCR System (BIO-RAD, United States). The amplification parameters were 95°C for 30 s, followed by 40 cycles of 95°C for 5 s and 60°C for 34 s, 95°C for 15 s, 60°C for 60 s, and 95°C for 15 s. The relative expression of mRNA was calculated by the $2^{-\Delta\Delta Ct}$ method after normalization to β-actin. All primer sequences used are listed in Table 1.

2.12 | Immunofluorescence staining

A slide coated with poly L-lysine (0.1 mg/ml) was placed in a 6-well plate. BV2 cells were cultured and treated as indicated, and fixed with 4% paraformaldehyde for 30 min at room temperature followed by permeabilization using 0.3% Triton X-100 for 15 min. After three rinses with PBS, the cells were blocked with 1% bovine serum albumin for 1 hr. The cells were incubated with rabbit anti-NF-kB p65 primary antibody (1:200 dilutions) at 4°C overnight. On the following day, the cells were washed with PBS three times and incubated with fluorescein isothiocyanate-conjugated goat anti-rabbit secondary antibody (1:400 dilutions) for 1 hr at room temperature. The cells were treated with an anti-fade mounting medium with DAPI for 10 min at 37°C in the dark. All images were captured with a fluorescence microscope (Olympus, Japan) and ×400 magnification.

2.13 | Flow cytometry analysis

Cells were plated in 6-well dishes at a density of 1×10^6 per well and incubated as aforementioned for 24 hr. The cells in the culture dish were digested using trypsin and then washed and re-suspended in cold PBS at a density of $(1–3) \times 10^6$ cells/ml. The membrane protein CD32 was detected by direct immunofluorescence staining. CD206 was fixed using fixation buffer and then permeabilized twice by intracellular staining perm wash buffer. Then, the cells were incubated with PE-conjugated monoclonal mouse CD32 antibodies or APC-conjugated monoclonal mouse CD206 antibodies at room temperature in the dark for 30 min. The cells were washed twice with PBS and re-suspended in 500 μl of 1 × PBS solution. APC and PE-conjugated monoclonal antibodies with irrelevant specificity were used as negative controls. The light scattering characteristics of each sample (10^5 cells) were analyzed using flow cytometer (CytoFLEX, Beckman Coulter, USA) equipped with FlowJo software (version vX 0.7).

2.14 | Molecular docking between compound and hub gene

The structure of ligand molecular was downloaded from the Traditional Chinese Medicine Systems Pharmacology Database and

TABLE 1 Primer sequences of qPCR

Gene	Forward primer	Reverse primer
β-Actin	CTACCTCATGAAGATCCTCACCGA	TTCTCCTTAATGTCACGCACGATT
IL10	CTTACTGACTGGCATGAGGATCA	GCAGCTCTAGGAGCATGTGG
IL1β	GAAATGCCACCTTTTGACAGTG	TGGA TGCTCTCATCAGGACAG
iNOS	GTTCTCAGCCCAACAATACAAGA	GTGGACGGGTCGATGTCAC
CD32	TGGACAGCCGTGCTAAATCTT	GGTCCCTTCGCATGTCAGTG
CD206	CTCTGTTCAGCTATTGGACGC	CGGAATTTCTGGGATTCAGCTTC
Arg-1	GCATATCTGCCAAAGACATCG	CTTCCATCACCTTGCCAATC
TNF-α	CTGAACTTCGGGGTGATCGG	GGCTTGTCACTCGAATTTTGAGA

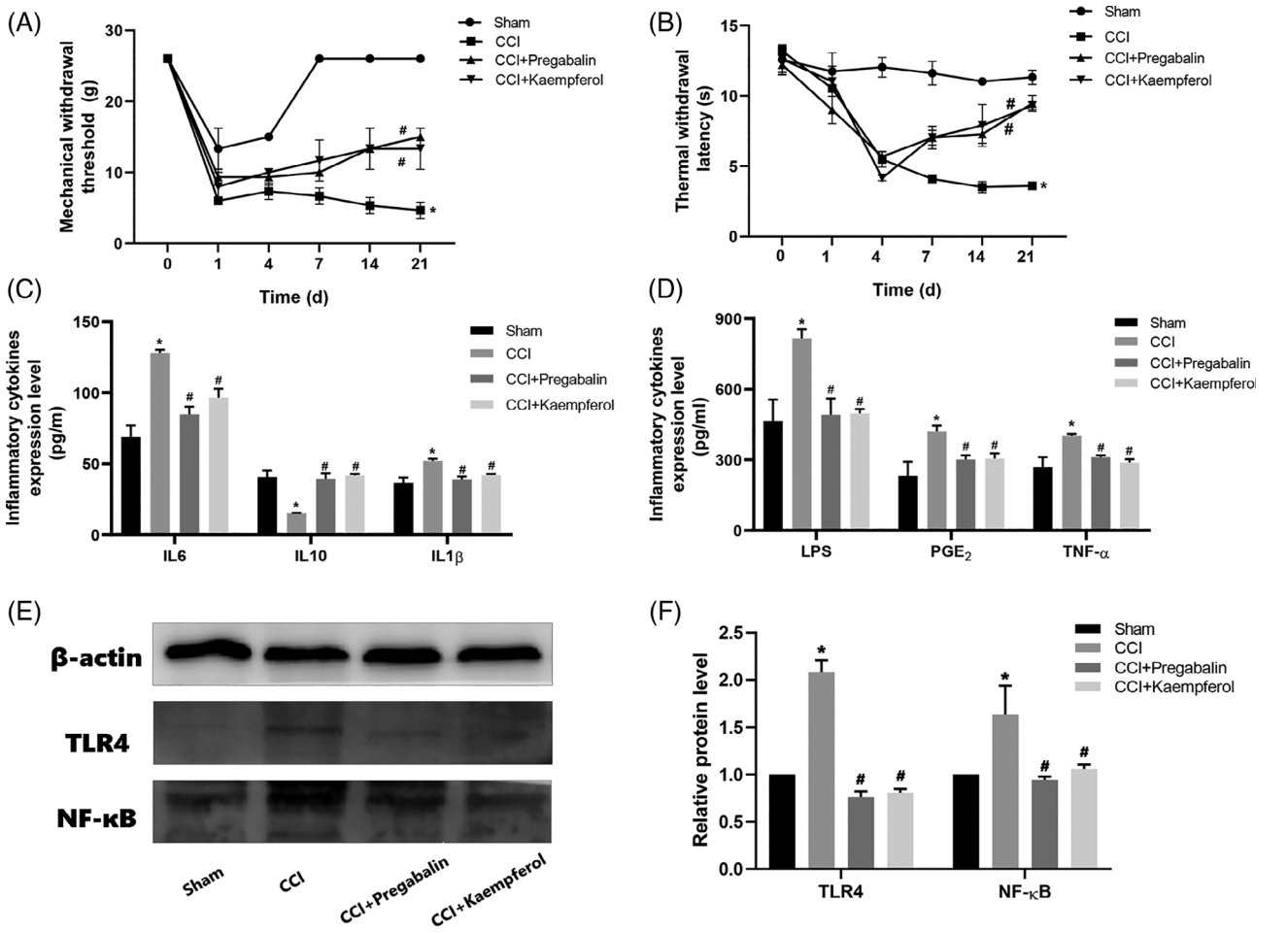

FIGURE 1 Kaempferol attenuated CCI-induced neuropathic pain. (a) PMWT and (b) PTWL were measured at 0, 1, 4, 7, 14, and 21 days before and after CCI induction. Kaempferol relieved CCI-induced inflammatory cytokines overexpression. (c) Levels of IL6, IL10, and IL1β measured by ELISA and (d) levels of LPS, PGE2, and TNF-α measured by ELISA. Kaempferol down-regulated CCI-induced overexpression of TLR4 and NF-κB protein. (e,f) TLR4 and NF-κB protein in rats spinal dorsal horn measured by western blotting. $n = 3$, $^*p < .05$ versus sham group, and $\#p < .05$ versus CCI group. One-way ANOVA was used to determine the difference between groups

Analysis Platform (TCMSP). The 3D protein structure was obtained from the RCSB PDB database (http://rcsb.org/). Then we used PyMol software to remove all water molecules in the protein 3D structure and added the polar hydrogen and Gasteiger charges to the protein and ligands with AutodockTools 1.5.6. At the same time, the docking box of the protein was predicted in Deepsite (https://www.playmolecule.com/deepsite/). Autodock Tools were applied to match compound and gene where Autodock Vina was employed to find the best docking condition. The docking energy was used to evaluate the result of molecular docking. Analysis and visualization of the docking results were realized by the PyMol.

2.15 | Statistical analyses

Each experiment was repeated successfully at least in triplicate. Statistical data are presented as means ± *SEM* and analyses were performed with SPSS 20.0 (IBM, NY) and GraphPad Prism 8 (GraphPad Software, CA) software. The significance of difference was assessed with one-way ANOVA followed by a post hoc (Bonferroni) test for multiple group comparisons if the data were normally distributed and homogenous. *p*-value of <.05 was considered statistically significant.

3 | RESULTS

3.1 | Kaempferol relieved neuropathic pain in CCI rats

As shown in Figure 1A,B, the PWMT and PWTL values of the CCI rats in the model group were significantly lower than those in the sham operation group ($p < .05$). However, compared with the CCI group, kaempferol treatment significantly increased the PWMT and PWTL values. Meanwhile, the PWMT and PWTL values in the Kae group were significantly lower than those in the Sham group ($p < .05$). These results indicated that kaempferol could alleviate NP in CCI rats.

3.2 | Inhibition of inflammatory cytokines by kaempferol

ELISA was used to investigate whether kaempferol regulated the expression of inflammatory cytokines in rat blood serum. The results showed (Figure 1C,D) that the level of pro-inflammatory cytokines was greatly increased by CCI stimulation, as demonstrated by the production of IL-1β, IL-6, LPS, TNF-α, and PGE2. The anti-inflammatory cytokines (IL-10) were decreased after CCI stimulation. Importantly, kaempferol treatment inhibited CCI-induced pro-inflammatory cytokine (IL-1β, IL-6, LPS, TNF-α, and PGE2) synthesis and stimulated IL-10 production.

3.3 | Effects of Kaempferol on sciatic nerve morphology and the expression of Iba1, S100b, and TLR4 in CCI rats

We observed from HE staining (Figure 2A) that the sciatic nerve structure in the sham operation group was complete, with no inflammatory cell infiltration and no Schwann cell proliferation; While in the CCI model group, it was observed that the sciatic nerve structure was destroyed, inflammatory cells infiltrated nerve fibers, and Schwann cells proliferated in large numbers. Both pregabalin and kaempferol reduced the number of inflammatory cells in the injured sciatic nerve and it partially recovered the tissue structure but obviously did not return to normal. After treatment, Schwann cell proliferation decreased compared with that of the CCI model group, and inflammatory cell infiltration decreased. Furthermore, immunohistochemical analysis showed (Figure 2B,C) that the expression of Iba1, S100b, and TLR4 in the CCI model rats was significantly higher than that in the sham group, and they distinctly decreased after treatment with kaempferol (Figure 2C, $p < .05$). All of these findings indicate that kaempferol could ameliorate pathological changes and inhibit TLR4 expression in the CCI rats. At the same time, we found both pregabalin and kaempferol intragastrical injection did not induce any obvious damage to rat liver (Figure 2E) and kidney (Figure 2F).

3.4 | Kaempferol down-regulated CCI-induced TLR4/NF-κB overexpression in rats spinal dorsal horn

Figure 1E,F shows that compared with the sham group, the protein expression of TLR4 and NF-κB p65 in the CCI model group was significantly increased ($p < .05$). However, the protein expression of TLR4 and NF-κB p65 in the spinal dorsal horn of CCI rats decreased obviously after pregabalin and kaempferol treatment ($p < .05$).

3.5 | Effects of kaempferol on the viability of BV2 cells

The results (Figure 3B) showed that kaempferol concentrations less than 100 μM did not induce any detectable cytotoxicity or influence BV2 cell viability but induced cytotoxicity at 250 μM concentration. Kaempferol at different concentrations (5, 10, and 50 μM) showed no significant toxic effects. We chose 10 μM as the dosing concentration.

3.6 | Kaempferol promoted microglial polarization to the M2 phenotype in LPS-induced BV2 cells

To determine the effects of kaempferol on LPS-induced inflammatory mediators, qRT-PCR was used to investigate whether kaempferol regulated the expression of inflammatory cytokines. The LPS-induced production of IL-1β, TNF-α, IL-10, iNOS, Arg-1, CD32, and CD206 was measured. The results showed (Figure 3C,D) that the level of M1 pro-inflammatory cytokines was strongly increased by LPS stimulation, as demonstrated by the production of IL-1β, TNF-α, iNOS, and CD32. M2 antiinflammatory cytokines (IL-10, Arg-1, and CD206) were decreased after LPS stimulation. Importantly, kaempferol treatment inhibited LPS-induced M1 pro-inflammatory cytokine (IL-1β, TNF-α, CD32, and iNOS) synthesis, whereas the production of M2 anti-inflammatory cytokines (IL-10, Arg-1, and CD206) was increased. These results indicate that kaempferol suppresses LPS-induced pro-inflammatory mediators and cytokine production in BV2 microglial cells. Consistent with our findings described above, kaempferol significantly decreased the LPS-induced IL-1β, TNF-α, iNOS, and CD32 mRNA levels (Figure 3C). In addition, treatment with TAK-242 and JSH-23 further decreased LPS-induced IL-1β, TNF-α, iNOS mRNA

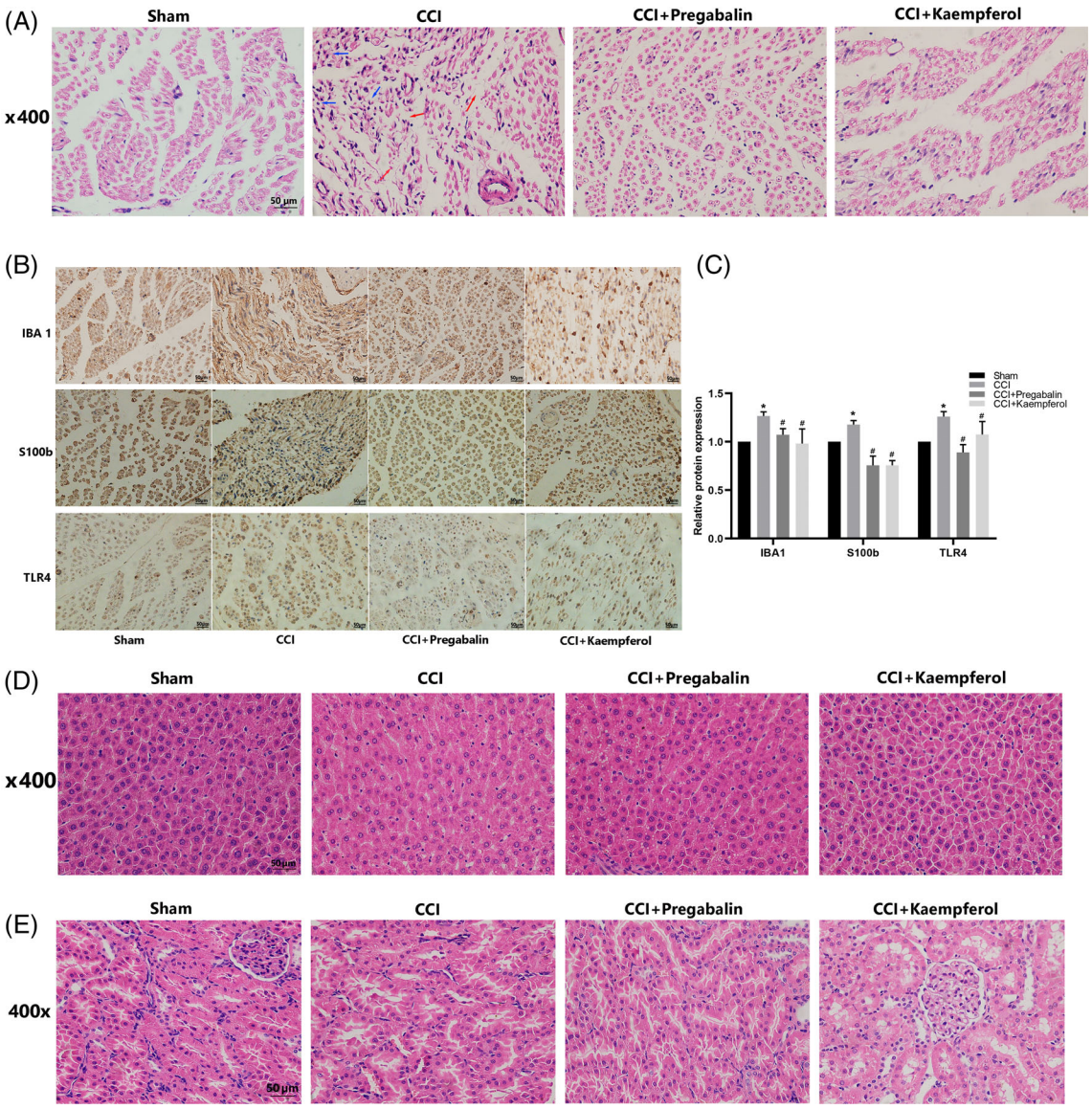

FIGURE 2 Kaempferol alleviated CCI-induced sciatic nerve damage. (a) H&E staining of rats right sciatic nerve, the blue arrows in the CCI group point out Schwann cells proliferation in large numbers and the red arrows point out that nerve structure was destroyed; (b,c) Iba-1, S100b, and TLR4 positive cells expressed in rats right sciatic nerve; $n = 3$,$^{*}p < .05$ versus sham group, $\#p < .05$ versus CCI group. (d) H&E staining of (e) rat liver and (f) rat kidney. Scale bar = 50 μm

levels compared with treatment with LPS. Conversely, treatment with TAK-242 and JSH-23 increased LPS-induced IL10, Arg-1, and CD206(Figure 3D). However, treatment with JSH-23 did not significantly reduce the LPS-induced CD32 mRNA levels compared (Figure 3C).

CD32 was used as a marker of M1 polarization, while CD206 was employed as a marker of M2 polarization. To further determine whether kaempferol switched microglial phenotype from M1 to M2 and to some extent exerted neuroprotective effect, we measured the expression of CD32 and CD206 via flow cytometry to determine the effect of kaempferol on phenotypic switching in BV2 cells. As shown in Figure 3E–H, higher levels of CD32 immunoreactivity (Figure 3E) and diminished CD206 immunoreactivity (Figure 3G) were detected in LPS-treated cultures than in the control group ($p < .05$). Kaempferol treatment decreased CD32 immunoreactivity and increased CD206 immunoreactivity ($p < .05$).

3.7 | Effects of kaempferol on TLR4/NF-κB pathways

TLR4 is a microglial membrane receptor that plays an important role in signaling pathways mediating inflammation. Because LPS may induce neuroinflammation via interactions with microglial membrane receptors, we first determined the levels of the key regulator-TLR4 in LPS-treated BV2 cells. As shown in Figure 4A, the western blot

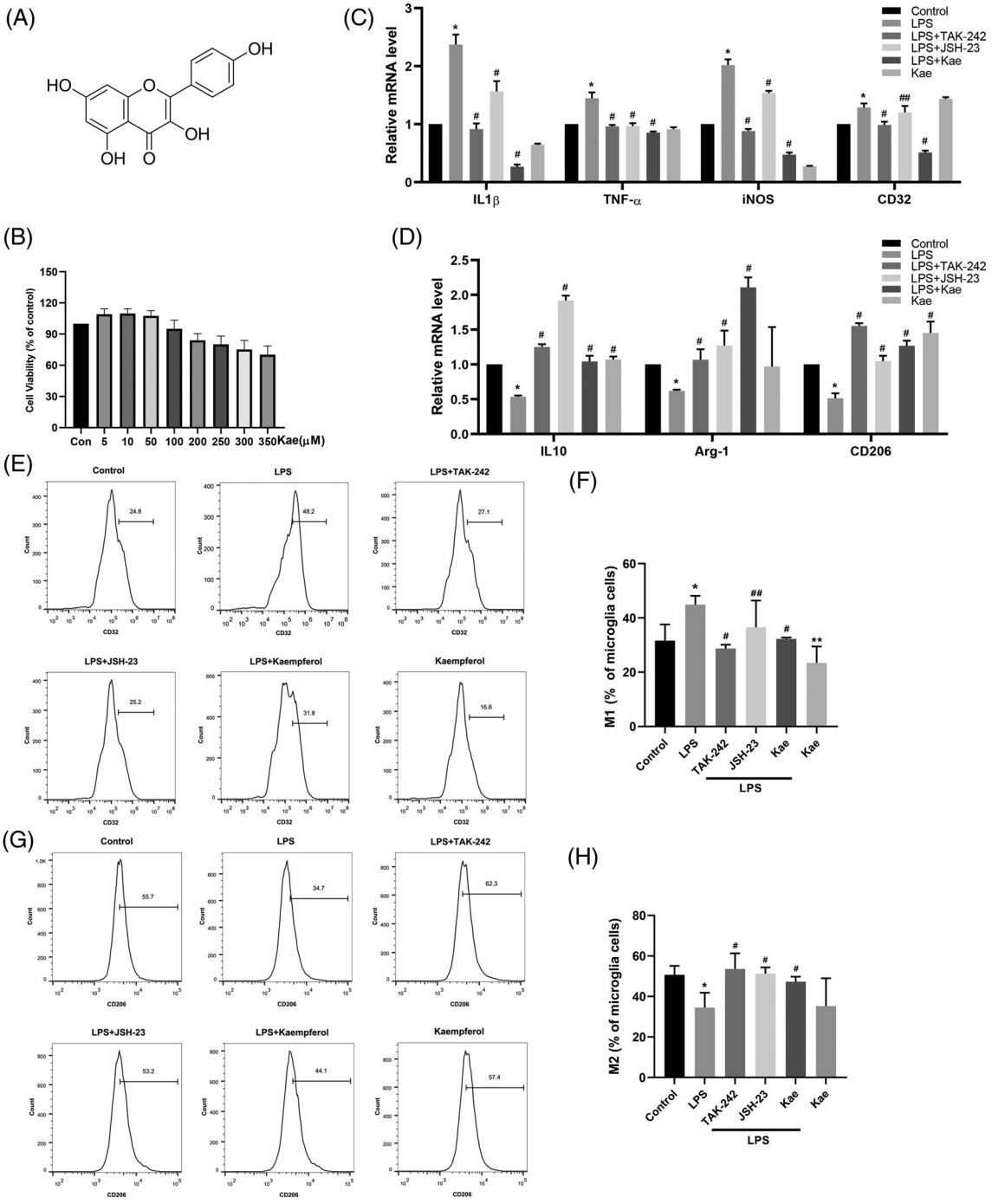

FIGURE 3 Effects of kaempferol on the survival of BV2 cells. (a) The chemical structure of kaempferol. (b) Cells were treated with 5–350 μM of kaempferol for 24 hr, and cell viability was determined by CCK8 assay. Kaempferol switched the increase of M1 polarization in LPS-induced BV2 cells and it stimulated the formation of the M2 phenotype. Same as TLR4/NF-κB inhibitor. (c) The relative levels of IL1β, TNF-α, iNOS, and CD32 (M1 markers) mRNA were measured by RT-PCR. (d) The relative levels of IL10, Arg-1, and CD206 (M2 markers) mRNA were measured by RT-PCR. Effects of kaempferol on M1/M2 polarization in LPS-induced BV2 cells. The proportion of M1 microglia (e,f) and the percentage of M2 microglia (g,h) were measured by flow cytometry. *$p < .05$ versus control group, #$p < .05$ versus LPS group, and ##$p > .05$ versus LPS group. One-way ANOVA was used to determine the difference between groups

showed a persistent upregulation of TLR4 expression in LPS-treated BV2 cells compared with the control group. However, kaempferol treatment effectively inhibited TLR4 expression. Because the activation of NF-κB by LPS induced the expression of proinflammatory cytokines, we evaluated the effects of kaempferol on the NF-κB pathway via western blotting analysis. As shown in Figure 4A,B, LPS stimulation resulted in the phosphorylation of NF-κB p65 without affecting the expression of NF-κB p65. However, kaempferol

treatment decreased the expression of p-NF-κB p65. Together, these results indicate that kaempferol abrogated the LPS-induced imbalance of TLR4 by affecting downstream NF-κB activation, which may probably contribute to the overactivation of microglial.

Interestingly, TAK-242 (a TLR4 inhibitor) and JSH-23 (an NF-κB inhibitor) prevented LPS-induced overexpression of these proteins (Figure 4A,B). Furthermore, LPS increased the p-NF-κB protein level, while kaempferol and JSH-23 (an NF-κB inhibitor) reduced its level significantly (Figure 4A,B).

The molecular docking maps were shown in Figure 4c as well as the binding sites of TLR4 protein. The scores for the Kae-TLR4 molecule-protein docking were -7.5 kcal mol^{-1}, suggesting that Kaempferol was tightly bound to TLR4. Kae formed a hydrogen bond with a bond length of 2.9, 3.0, and 2.5 Å in TLR4 protein amino acids ASP100, ASP99, and GLU229, respectively (Figure 4C).

3.8 | Kaempferol inhibits LPS-induced JNK, ERK, and p38 MAPK phosphorylation

We investigated the effects of kaempferol on the activation of ERK1/2, JNK, and p38 MAPK in LPS-stimulated BV2 cells. As shown in Figure 5A–D, LPS strongly activated ERK, JNK, and p38 MAPK (their phosphorylated forms, pERK, pJNK, pP38 MAPK are shown) whereas ERK and JNK were slightly activated. Kaempferol had significant inhibitory effects on LPS-stimulated ERK, JNK, and p38 MAPK activation.

3.9 | Kaempferol attenuates LPS-induced NF-kB activation in BV2 cells

NF-κB activation involves the translocation of the p65 subunit of NF-κB into the nucleus. Thus, we investigated whether kaempferol inhibits p65 nuclear translocation. Figure 4D,E show that the nuclear phosphorylation level of NF-κB p65 was increased by LPS while TAK-242, JSH-23, and kaempferol all inhibited the cell nuclear activation. Immunofluorescence analysis showed that the p65 protein was primarily located in the cytosol during the untreated condition. When BV2 cells were exposed to LPS, the p65 protein moved into the nuclei, and the BV2 cells changed their morphology (Figure 6). Kaempferol treatment reduced the p65 nuclear immunoreactivity, as well as the morphological change induced by LPS. Interestingly, we further examined whether NF-kB activation is involved in the signal

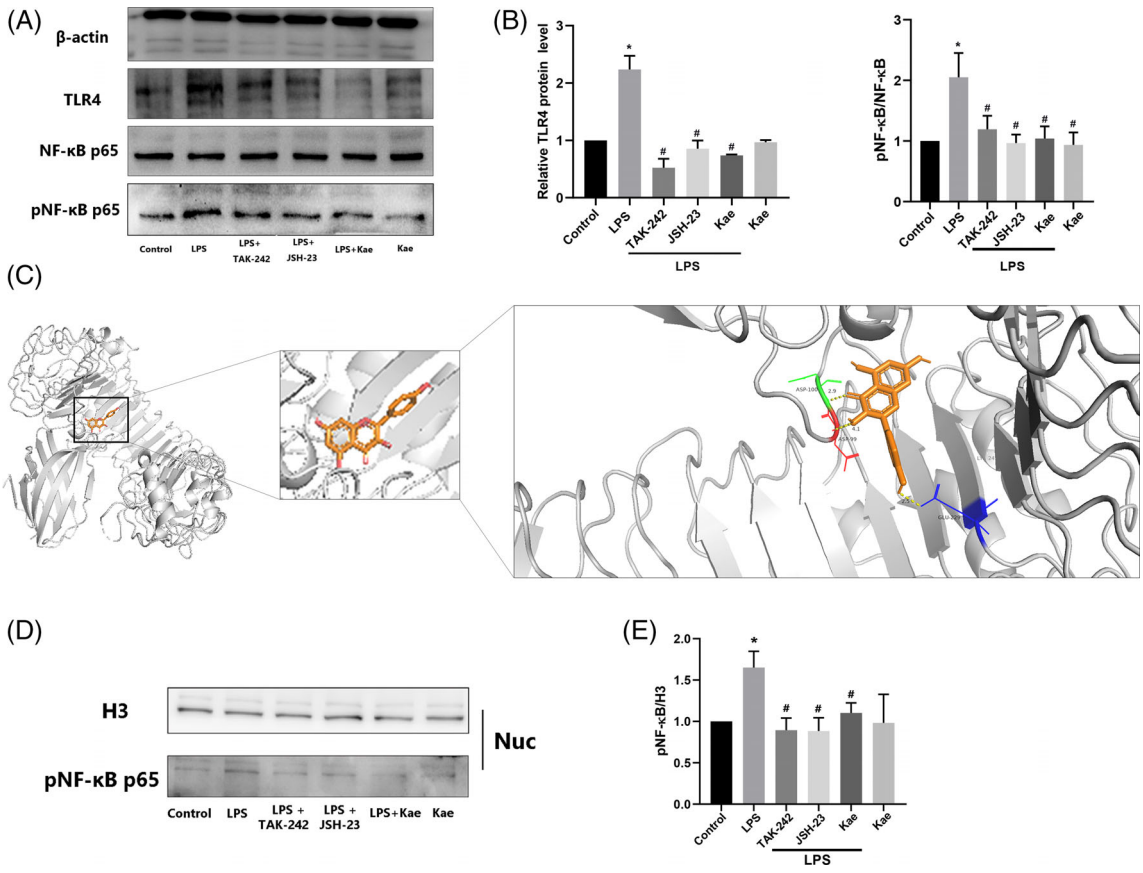

FIGURE 4 Kaempferol inhibited LPS-induced inflammation in BV2 cells through TLR4/NF-κB signaling pathway. (a–b) TLR4, NF-κB, and p-NF-κB protein level measured by western blotting. (c) The molecular docking prediction between kaempferol and TLR4 protein, (d,e) kaempferol inhibited LPS-induced nuclear p-p65 activation. $n = 3$, $^*p < .05$ versus control group, and $\#p < .05$ versus LPS group. One-way ANOVA was used to determine the difference between groups

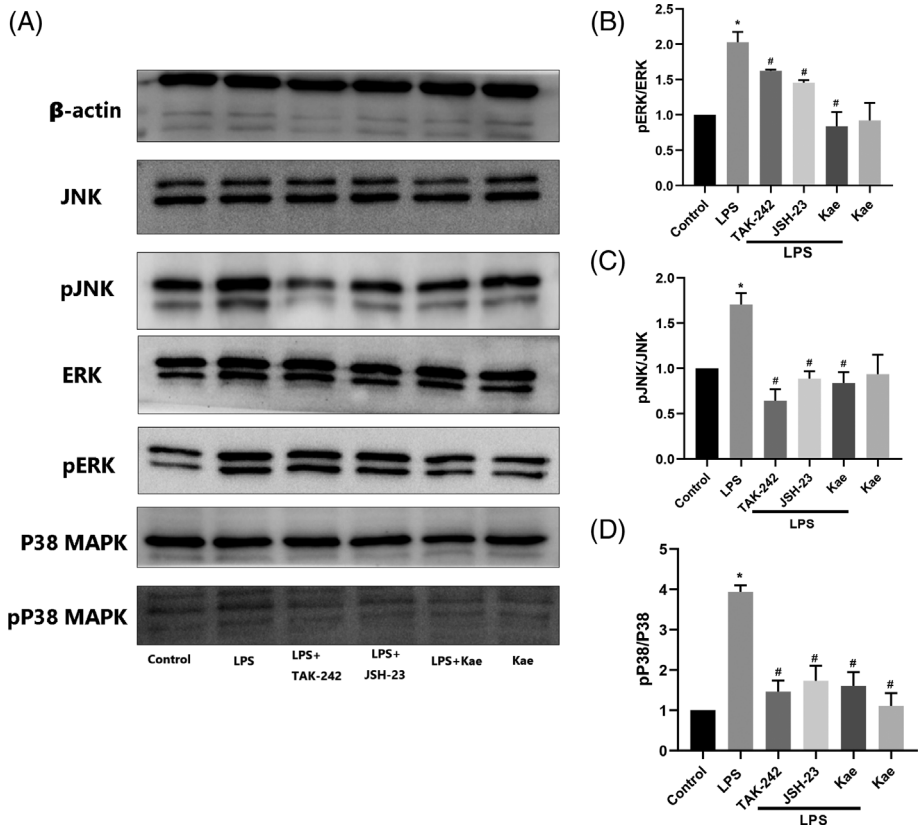

FIGURE 5 Inhibitory effects of kaempferol on LPS-induced JNK, ERK, and p38 MAPK activation in BV2 cells. (a–d) JNK, pJNK, ERK, pERK, p38 MAPK, and p p38 MAPK protein level measured by western blotting. $n = 3$,*$p < .05$ versus control group, and #$p < .05$ versus LPS group. One-way ANOVA was used to determine the difference between groups

transduction pathway caused by the NF-kB inhibitor JSH-23. Figure 6 shows that JSH-23 (10 μM) reduced p65 nuclear immunoreactivity, similar to the TLR4 inhibitor (TAK-242).

4 | DISCUSSION

In recent years, several phytochemicals have been comprehensively investigated for their potential neuroprotective effects in various neurological disorders (Kim et al., 2019; Patel & Udayabanu, 2017). Flavonoids possess a wide range of health-promoting properties and are indispensable components in various pharmaceutical, cosmetics, nutraceutical, and medicinal applications. They can modulate the functions of key cellular enzymes as well as provide direct antioxidant and antiinflammatory effects (Panche, Diwan, & Chandra, 2016). Kaempferol is a polyphenol that is richly found in fruits and vegetables (Figure 3A). It has been shown that kaempferol is involved in inhibiting various enzymes that provoke the inflammation process induced by mediators such as prostaglandins and nitric oxide production (Alam, Khan, Shah, Cauli, & Saso, 2020).

Neuroinflammation leads to chronic pain by regulating the infiltration of immune cells, the activation of glial cells (mainly microglial and astrocytes), and the production of inflammatory mediators in the peripheral and central nervous system (Calvo, Dawes, & Bennett, 2012). Neuroinflammation mediated by microglial is considered to be an important pathological process associated with NP (Ellis & Bennett, 2013).

Activation of microglial is one of the universal components of neuroinflammation. In this study, we explored the anti-inflammatory properties of kaempferol against CCI in vivo or LPS in vitro-induced neuroinflammation by regulating microglial M1/M2 polarization by down-regulating the TLR4/NF-κB signaling pathway.

Microglial are activated in response to nerve injury and then they release proinflammatory cytokines such as TNF-α, IL-1β, and IL-6, thus initiating the NP process. ELISA measuring inflammation markers such as TNF-α, IL-1β, IL-6, PGE2, and LPS in rat blood serum indicated that kaempferol treatment could reduce inflammation compared with the CCI model group (Figure 1C,D, $p < .05$). The H&E staining and immunohistochemistry results all showed that compared with the sham operation group, the sciatic nerve of rats in the CCI group was more obviously damaged, and therefore, an inflammation reaction was generated. While kaempferol treatment effectively alleviated the pain caused by CCI, and 21 days of treatment significantly reduced inflammation (Figure 1).

The Iba-1 antibody is generally used to detect microglial activation after peripheral nerve injury via immunocytochemical staining (Ahmed et al., 2007). S100b is a helix–loop–helix protein with a calcium-binding domain associated with various neurological disorders through activation of the MAPK pathway, increasing NF-κB expression resulting in cell survival, proliferation, and gene up-regulation. The S100b protein plays a crucial role in Alzheimer's disease, Parkinson's disease, multiple sclerosis, and epilepsy because high expression of this protein directly targets astrocytes and promotes neuroinflammation. Increased levels of S100b are useful for assessing

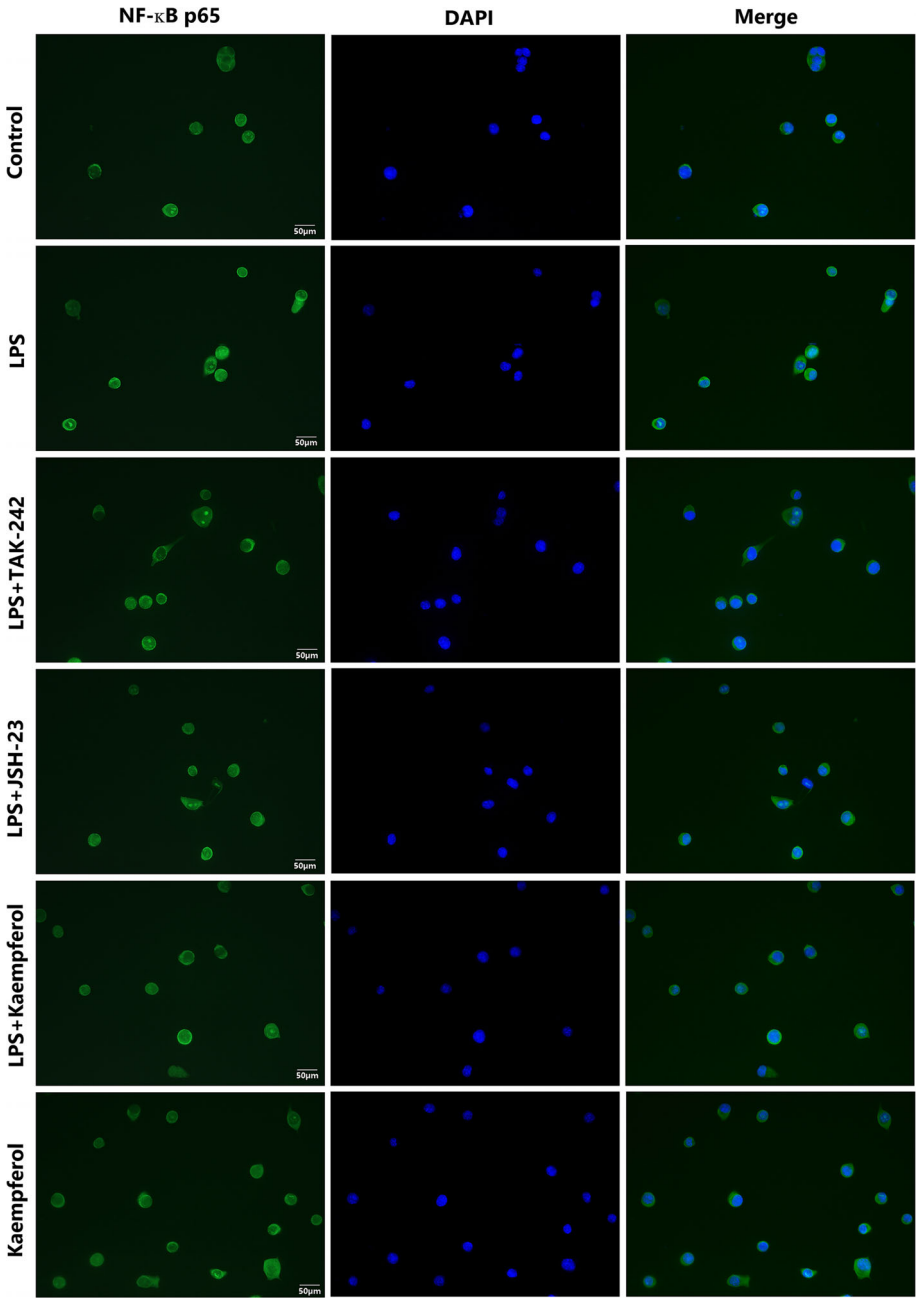

FIGURE 6 Inhibition of LPS-induced NF-κB activation by kaempferol in BV2 cells. The translocation of the p65 subunit of NF-κB was determined by immunofluorescence. Representative pictures from three independent experiments are shown. Scale bar = 50 μm

the release of inflammatory markers, and excitotoxicity-dependent neuronal loss (Langeh & Singh, 2021). Immunohistochemistry of the sciatic nerve showed there were numerous Iba-1, S100b, and TLR4-positive cells in the CCI model group while kaempferol treatment group distinctly reduced the numbers of these positive cells (Figure 2B,C).

The M1 phenotype was originally induced by LPS or interferon (IFN)-γ stimulation and characterized by increased expression of several proteins or cytokines, such as iNOS, CD32, CD68, IL-1β, IL-6, and TNF-α. The M2 phenotype is induced by IL-4, or IL-10 and is characterized by increased expression of several proteins or cytokines, such as Arg-1, mannose receptor (MR/CD206), IL-4, and IL-10 (Ruytinx, Proost, Van Damme, & Struyf, 2018). IL-10 is an anti-inflammatory cytokine. It is slowly but continuously increased following nerve injury, which may be a compensatory and protective mechanism targeting the increase of pro-inflammatory cytokines. Wang et al. found in their study that DUSP1 switched microglial M1 to M2 polarization in the mPFC and attenuated CCI-induced NP by inhibiting MAPK signaling, suggesting that microglial M2 polarization is involved in the analgesic effect of DUSP1, which might represent a promising target to treat NP (Wang et al., 2021). It has been reported that the analgesic effects of koumine on CCI-induced NP may result from the inhibition of microglial activation and M1 polarization as well as the activation of astrocytes while sparing the antiinflammatory responses to NP (Jin et al., 2018).

To further investigate the effect of kaempferol on microglial M1/M2 polarization, LPS-induced BV2 microglial were used. Our

results showed that kaempferol reduced the mRNA expression of M1 markers (CD32, IL-6, IL-1β, TNF-α, and iNOS) in LPS-induced BV2 microglial cells and that the upregulation of anti-inflammatory cytokines (IL10, CD206, and Arg-1) indicates that kaempferol may act at the transcriptional level to inhibit microglial M1 polarization (Figure 3C, $p < .05$). Flow cytometry experimental results corroborated this speculation in that the data showed that treatment with kaempferol significantly counteracted the influence LPS had on microglial M1 polarization, as demonstrated by a decrease in the percentage of M1 microglial (Figure 3F), and the expression of M1 markers (CD32) (Figure 3E), and an increase in the percentage of M2 microglial (Figure 3H) and the expression of M2 markers (CD206).

TLRs act principally to initiate an innate immune response, and inflammation is the central hallmark of this response. Systemic inflammation induced by TLRs results primarily from the activation of macrophages and neutrophils, cell types with specialized functions in innate immunity. TLR ligands cause macrophages to produce inflammatory cytokines such as TNF-α, IL-1, and IL-6 (Moresco, LaVine, & Beutler, 2011). TNF-α, IL-1β, and IL-10 are the downstream inflammatory cytokines of the TLR4 signaling pathway. Michela et al. clearly demonstrated that the absence of TLR4 reduces the development of neuroinflammation associated with PD through NF-κB, AP-1, and inflammasome pathways modulation (Campolo et al., 2019). Curcumin significantly alleviates LPS-induced inflammation by regulating microglial (M1/M2) polarization by reducing the imbalance of TREM2 and TLR4 and balancing the downstream NF-κB activation (J. Zhang et al., 2019). Hesperetin attenuates the neuroinflammation-mediated neurodegeneration, cognitive and learning decline, and memory impairments by regulating the TLR4/NF-κB signaling pathway against the detrimental effects of LPS (Muhammad, Ikram, Ullah, Rehman, & Kim, 2019). It has been reported that intrathecal injection of epigallocatechin gallate, a TLR4 inhibitor, as well as a kind of flavonoids derived from green tea, exerted obvious neuroprotective effects reflecting in that the expressions of TLR4, NF-κB, HMGB1, TNF-α, and IL-1β were markedly decreased while the content of IL-10 in the spinal cord increased significantly accompanied by dramatical improvement of pain behaviors in CCI rats (Kuang et al., 2012). Discoveries all imply that the TLR4 signaling pathway plays an important role in the occurrence and development of NP, and is a promising therapeutic target. To further validate whether kaempferol treatment promotes microglial M2 polarization through the TLR4/NF-κB signaling pathway, we treated BV2 cells with a TLR4 inhibitor (TAK-242) or an NF-κB inhibitor (JSH-23) in the presence of LPS. TAK-242 (resatorvid), a small-molecule-specific inhibitor of TLR4 signaling, inhibits the production of lipopolysaccharide-induced inflammatory mediators by binding to the intracellular domain of TLR4 (Matsunaga, Tsuchimori, Matsumoto, & Ii, 2011). JSH-23 (4-methyl-N 1-[3-phenylpropyl]-benzene-1,2-diamine) is a novel chemical synthetic compound. The aromatic diamine JSH-23 compound has an inhibitory effect on NF-κB transcriptional activity in LPS-stimulated RAW 264.7 macrophages and it interferes LPS-induced nuclear translocation of NF-κB without affecting IκB degradation through a rare mechanism of action for controlling NF-κB activation (Shin et al., 2004). Levels of TLR4/NF-κB protein expression measured by western blot clearly demonstrated that LPS-induced TLR4 activation was dramatically reversed by kaempferol, similar to TAK-242 or JSH-23 treatment (Figure 4A), indicating that it blocks the activation of this sensor molecule of the neuroinflammatory pathway. NF-κB activation involves the translocation of the p65 subunit of NF-kB into the nucleus. The p65 protein was primarily located in the cytosol under untreated conditions. When BV2 cells were exposed to LPS, the p65 protein appeared in nuclei, and BV2 cells changed their morphology, while TAK-242, JSH-23, and kaempferol all inhibited its translocation (Figure 6).

The activation of the NF-κB pathway causes the synthesis and release of proinflammatory cytokines, including TNF-α, IL-6, and IL-1β which may play a pivotal role in neuroinflammation while the activation of the MAPK pathway may play an important role in the regulation of neuronal plasticity. The MAPK pathway includes a number of proteins, such as p38, ERK, and JNK, which are involved in many facets of cellular regulation, from gene expression to cell death (Chang & Karin, 2001). The TLR4-induced MAPK pathway can initiate immune and inflammatory responses, defending against harmful stimuli (P. Zhang, Yang, et al., 2020). The p38 MAPK pathway has also been linked to microglial activation and contributes to postoperative thermal hyperalgesia and mechanical allodynia in rats (Horvath, Landry, Romero-Sandoval, & DeLeo, 2010). Following TLR4 activation, a MyD88-independent pathway can be activated. This culminates in MAPK signaling and activation of the transcription factor NF-κB (Okun et al., 2009). It has been reported that JNK is an essential mediator of several proinflammatory stimuli in microglial, and intervention in this pathway may be a therapeutic approach for treating inflammatory neurological diseases (Waetzig et al., 2005). It has been reported that Kaempferol is able to reduce LPS-induced inflammatory mediators through the down-regulation of TLR4, NF-κB, p38 MAPK, JNK, and AKT suggesting that kaempferol has therapeutic potential for the treatment of neuroinflammatory diseases (Park, Sapkota, Kim, Kim, & Kim, 2011).

In this study, we further examined the involvement of the MAPK signaling pathway in the antiinflammatory effects of kaempferol. The results revealed that kaempferol inhibited LPS-induced activation of p38 MAPK, JNK, and ERK in BV2 cells, which have been reported to be involved in inflammatory mediator production in response to a wide variety of stimuli, including LPS. Both TLR4 and NF-κB inhibition further blocked the LPS-induced phosphorylation of ERK1/2, JNK, and p38 MAPK (Figure 5). Our microglial conditioned media results indicate that kaempferol can be neuroprotective by suppressing microglial activation.

5 | CONCLUSION

The analgesic effects of kaempferol on CCI-induced NP may result from inhibition of microglial activation and switching the M1 to M2 phenotype while sparing anti-inflammatory responses.

ACKNOWLEDGMENTS

This work was supported by the National Natural Science Foundation of China (No. 81874404).

CONFLICT OF INTEREST

The authors declare no conflicts of interest.

DATA AVAILABILITY STATEMENT

The data that support the findings of this study are available from the corresponding author upon reasonable request.

ORCID

Shiquan Chang https://orcid.org/0000-0003-3888-9282
Di Zhang https://orcid.org/0000-0001-9134-6573

REFERENCES

Ahmed, Z., Shaw, G., Sharma, V. P., Yang, C., McGowan, E., & Dickson, D. W. (2007). Actin-binding proteins coronin-1a and IBA-1 are effective microglial markers for immunohistochemistry. *The Journal of Histochemistry and Cytochemistry: Official Journal of the Histochemistry Society*, *55*(7), 687–700. https://doi.org/10.1369/jhc.6A7156.2007

Alam, W., Khan, H., Shah, M. A., Cauli, O., & Saso, L. (2020). Kaempferol as a dietary anti-inflammatory agent: Current therapeutic standing. *Molecules (Basel, Switzerland)*, *25*(18), 4073. https://doi.org/10.3390/molecules25184073

Attal, N. (2001). Pharmacologic treatment of neuropathic pain. *Acta Neurologica Belgica*, *101*(1), 53–64.

Baron, R. (2006). Mechanisms of disease: Neuropathic pain--a clinical perspective. *Nature Clinical Practice. Neurology*, *2*(2), 95–106. https://doi.org/10.1038/ncpneuro0113

Baron, R., Binder, A., & Wasner, G. (2010). Neuropathic pain: Diagnosis, pathophysiological mechanisms, and treatment. *The Lancet Neurology*, *9*(8), 807–819. https://doi.org/10.1016/S1474-4422(10)70143-5

Calvo, M., Dawes, J. M., & Bennett, D. L. (2012). The role of the immune system in the generation of neuropathic pain. *The Lancet Neurology*, *11*(7), 629–642. https://doi.org/10.1016/S1474-4422(12)70134-5

Campolo, M., Paterniti, I., Siracusa, R., Filippone, A., Esposito, E., & Cuzzocrea, S. (2019). TLR4 absence reduces neuroinflammation and inflammasome activation in Parkinson's diseases in vivo model. *Brain, Behavior, and Immunity*, *76*, 236–247. https://doi.org/10.1016/j.bbi.2018.12.003

Chang, L., & Karin, M. (2001). Mammalian MAP kinase signalling cascades. *Nature*, *410*(6824), 37–40. https://doi.org/10.1038/35065000

Colloca, L., Ludman, T., Bouhassira, D., Baron, R., Dickenson, A. H., Yarnitsky, D., … Raja, S. N. (2017). Neuropathic pain. *Nature Reviews Disease Primers*, *3*, 17002. https://doi.org/10.1038/nrdp.2017.2

Dai, W. L., Bao, Y. N., Fan, J. F., Li, S. S., Zhao, W. L., Yu, B. Y., & Liu, J. H. (2020). Levo-corydalmine attenuates microglia activation and neuropathic pain by suppressing ASK1-p38 MAPK/NF-κB signaling pathways in rat spinal cord. *Regional Anesthesia and Pain Medicine*, *45*(3), 219–229. https://doi.org/10.1136/rapm-2019-100875

Ellis, A., & Bennett, D. L. (2013). Neuroinflammation and the generation of neuropathic pain. *British Journal of Anaesthesia*, *111*(1), 26–37. https://doi.org/10.1093/bja/aet128

Harden, R. N. (1999). Gabapentin: A new tool in the treatment of neuropathic pain. *Acta Neurologica Scandinavica. Supplementum*, *173*, 43–52. https://doi.org/10.1111/j.1600-0404.1999.tb07389.x

Hargreaves, K., Dubner, R., Brown, F., Flores, C., & Joris, J. (1988). A new and sensitive method for measuring thermal nociception in cutaneous hyperalgesia. *Pain*, *32*(1), 77–88. https://doi.org/10.1016/0304-3959(88)90026-7

Horvath, R. J., Landry, R. P., Romero-Sandoval, E. A., & DeLeo, J. A. (2010). Morphine tolerance attenuates the resolution of postoperative pain and enhances spinal microglial p38 and extracellular receptor kinase phosphorylation. *Neuroscience*, *169*(2), 843–854. https://doi.org/10.1016/j.neuroscience.2010.05.030

Inoue, K., & Tsuda, M. (2018). Microglia in neuropathic pain: Cellular and molecular mechanisms and therapeutic potential. *Nature Reviews. Neuroscience*, *19*(3), 138–152. https://doi.org/10.1038/nrn.2018.2

Jin, G. L., He, S. D., Lin, S. M., Hong, L. M., Chen, W. Q., Xu, Y., … Yu, C. X. (2018). Koumine attenuates neuroglia activation and inflammatory response to neuropathic pain. *Neural Plasticity*, *2018*, 9347696. https://doi.org/10.1155/2018/9347696

Kim, S. Y., Jin, C. Y., Kim, C. H., Yoo, Y. H., Choi, S. H., Kim, G. Y., … Choi, Y. H. (2019). Isorhamnetin alleviates lipopolysaccharide-induced inflammatory responses in BV2 microglia by inactivating NF-κB, blocking the TLR4 pathway and reducing ROS generation. *International Journal of Molecular Medicine*, *43*(2), 682–692. https://doi.org/10.3892/ijmm.2018.3993

Kuang, X., Huang, Y., Gu, H. F., Zu, X. Y., Zou, W. Y., Song, Z. B., & Guo, Q. L. (2012). Effects of intrathecal epigallocatechin gallate, an inhibitor of Toll-like receptor 4, on chronic neuropathic pain in rats. *European Journal of Pharmacology*, *676*(1–3), 51–56. https://doi.org/10.1016/j.ejphar.2011.11.037

Langeh, U., & Singh, S. (2021). Targeting S100B protein as a surrogate biomarker and its role in various neurological disorders. *Current Neuropharmacology*, *19*(2), 265–277. https://doi.org/10.2174/1570159X18666200729100427

Le, W., Rowe, D., Xie, W., Ortiz, I., He, Y., & Appel, S. H. (2001). Microglial activation and dopaminergic cell injury: An in vitro model relevant to Parkinson's disease. *The Journal of Neuroscience: The Official Journal of the Society for Neuroscience*, *21*(21), 8447–8455. https://doi.org/10.1523/JNEUROSCI.21-21-08447.2001

Lee, M. B., Lee, J. H., Hong, S. H., You, J. S., Nam, S. T., Kim, H. W., … Choi, W. S. (2017). JQ1, a BET inhibitor, controls TLR4-induced IL-10 production in regulatory B cells by BRD4-NF-κB axis. *BMB Reports*, *50*(12), 640–646. https://doi.org/10.5483/bmbrep.2017.50.12.194

Li, W. H., Cheng, X., Yang, Y. L., Liu, M., Zhang, S. S., Wang, Y. H., & Du, G. H. (2019). Kaempferol attenuates neuroinflammation and blood brain barrier dysfunction to improve neurological deficits in cerebral ischemia/reperfusion rats. *Brain Research*, *1722*, 146361. https://doi.org/10.1016/j.brainres.2019.146361

Lurie, D. I. (2018). An integrative approach to neuroinflammation in psychiatric disorders and neuropathic pain. *Journal of Experimental Neuroscience*, *12*, 1179069518793639. https://doi.org/10.1177/1179069518793639

Matsunaga, N., Tsuchimori, N., Matsumoto, T., & Ii, M. (2011). TAK-242 (resatorvid), a small-molecule inhibitor of toll-like receptor (TLR) 4 signaling, binds selectively to TLR4 and interferes with interactions between TLR4 and its adaptor molecules. *Molecular Pharmacology*, *79*(1), 34–41. https://doi.org/10.1124/mol.110.068064

Mitrirattanakul, S., Ramakul, N., Guerrero, A. V., Matsuka, Y., Ono, T., Iwase, H., … Spigelman, I. (2006). Site-specific increases in peripheral cannabinoid receptors and their endogenous ligands in a model of neuropathic pain. *Pain*, *126*(1-3), 102–114. https://doi.org/10.1016/j.pain.2006.06.016

Moresco, E. M., LaVine, D., & Beutler, B. (2011). Toll-like receptors. *Current Biology*, *21*(13), R488–R493. https://doi.org/10.1016/j.cub.2011.05.039

Muhammad, T., Ikram, M., Ullah, R., Rehman, S. U., & Kim, M. O. (2019). Hesperetin, a citrus flavonoid, attenuates LPS-induced neuroinflammation, apoptosis and memory impairments by modulating TLR4/NF-κB signaling. *Nutrients*, *11*(3), 648. https://doi.org/10.3390/nu11030648

Okun, E., Griffioen, K. J., Lathia, J. D., Tang, S. C., Mattson, M. P., & Arumugam, T. V. (2009). Toll-like receptors in neurodegeneration. *Brain Research Reviews*, *59*(2), 278–292. https://doi.org/10.1016/j.brainresrev.2008.09.001

Panche, A. N., Diwan, A. D., & Chandra, S. R. (2016). Flavonoids: An overview. *Journal of Nutritional Science*, *5*, e47. https://doi.org/10.1017/jns.2016.41

Park, S. E., Sapkota, K., Kim, S., Kim, H., & Kim, S. J. (2011). Kaempferol acts through mitogen-activated protein kinases and protein kinase B/AKT to elicit protection in a model of neuroinflammation in BV2 microglial cells. *British Journal of Pharmacology*, *164*(3), 1008–1025. https://doi.org/10.1111/j.1476-5381.2011.01389.x

Patel, S. S., & Udayabanu, M. (2017). Effect of natural products on diabetes associated neurological disorders. *Reviews in the Neurosciences*, *28*(3), 271–293. https://doi.org/10.1515/revneuro-2016-0038

Ruytinx, P., Proost, P., Van Damme, J., & Struyf, S. (2018). Chemokine-induced macrophage polarization in inflammatory conditions. *Frontiers in Immunology*, *9*, 1930. https://doi.org/10.3389/fimmu.2018.01930

Shin, H. M., Kim, M. H., Kim, B. H., Jung, S. H., Kim, Y. S., Park, H. J., … Kim, Y. (2004). Inhibitory action of novel aromatic diamine compound on lipopolysaccharide-induced nuclear translocation of NF-kappaB without affecting IkappaB degradation. *FEBS Letters*, *571*(1–3), 50–54. https://doi.org/10.1016/j.febslet.2004.06.056

Suzumura, A. (2013). Neuron-microglia interaction in neuroinflammation. *Current Protein & Peptide Science*, *14*(1), 16–20. https://doi.org/10.2174/1389203711314010004

Waetzig, V., Czeloth, K., Hidding, U., Mielke, K., Kanzow, M., Brecht, S., … Hanisch, U. K. (2005). c-Jun N-terminal kinases (JNKs) mediate pro-inflammatory actions of microglia. *Glia*, *50*(3), 235–246. https://doi.org/10.1002/glia.20173

Wang, X., Jiang, Y., Li, J., Wang, Y., Tian, Y., Guo, Q., & Cheng, Z. (2021). DUSP1 promotes microglial polarization toward M2 phenotype in the medial prefrontal cortex of neuropathic pain rats via inhibition of MAPK pathway. *ACS Chemical Neuroscience*, *12*(6), 966–978. https://doi.org/10.1021/acschemneuro.0c00567

Xu, N., Tang, X. H., Pan, W., Xie, Z. M., Zhang, G. F., Ji, M. H., … Zhou, Z. Q. (2017). Spared nerve injury increases the expression of microglia M1 markers in the prefrontal cortex of rats and provokes depression-like behaviors. *Frontiers in Neuroscience*, *11*, 209. https://doi.org/10.3389/fnins.2017.00209

Zhang, D., Sun, J., Yang, B., Ma, S., Zhang, C., & Zhao, G. (2020). Therapeutic effect of *Tetrapanax papyriferus* and hederagenin on chronic neuropathic pain of chronic constriction injury of sciatic nerve rats based on KEGG pathway prediction and experimental verification. *Evidence-Based Complementary and Alternative Medicine*, *2020*, 2545806. https://doi.org/10.1155/2020/2545806

Zhang, J., Zheng, Y., Luo, Y., Du, Y., Zhang, X., & Fu, J. (2019). Curcumin inhibits LPS-induced neuroinflammation by promoting microglial M2 polarization via TREM2/ TLR4/NF-κB pathways in BV2 cells. *Molecular Immunology*, *116*, 29–37. https://doi.org/10.1016/j.molimm.2019.09.020

Zhang, P., Yang, M., Chen, C., Liu, L., Wei, X., & Zeng, S. (2020). Toll-like receptor 4 (TLR4)/opioid receptor pathway crosstalk and impact on opioid analgesia, immune function, and gastrointestinal motility. *Frontiers in Immunology*, *11*, 1455. https://doi.org/10.3389/fimmu.2020.01455

How to cite this article: Chang, S., Li, X., Zheng, Y., Shi, H., Zhang, D., Jing, B., Chen, Z., Qian, G., & Zhao, G. (2022). Kaempferol exerts a neuroprotective effect to reduce neuropathic pain through TLR4/NF-κB signaling pathway. *Phytotherapy Research*, *36*(4), 1678–1691. https://doi.org/10.1002/ptr.7396